DOI: 10.1002/cmdc.200800433

Design, Synthesis, and Evaluation of Carnosine Derivatives as Selective and Efficient Sequestering Agents of Cytotoxic Reactive Carbonyl Species

Giulio Vistoli,[a] Marica Orioli,[a] Alessandro Pedretti,[a] Luca Regazzoni,[a] Renato Canevotti,[b] Gianpaolo Negrisoli,[b] Marina Carini,[a] and Giancarlo Aldini*[a]

Reactive carbonyl species (RCS) are important cytotoxic mediators generated by lipid oxidation of polyunsaturated fatty acids (PUFAs) and represent a novel drug target, as they are presumed to play a pathogenic role in several diseases. L-Carnosine (L-CAR, β-alanyl-L-histidine) is a specific detoxifying agent of RCS, but is rapidly hydrolyzed in human serum by carnosinase, a specific dipeptidase. Herein we describe the in silico design, synthesis, and biological evaluation of carnosine derivatives that are resistant to carnosinase and that have increased quenching efficacy. Stability against carnosinase-mediated turnover was achieved by isomerization of the histidine residue, leading to D-carnosine (D-CAR, β-alanyl-D-histidine), which maintains the same quenching activity of L-carnosine. A molecular modeling approach was then used to design derivatives characterized by an increased quenching efficacy. The most promising candidates were synthesized, and their stability and quenching activity were evaluated. This study describes a set of aryl derivatives that are characterized by high stability in human plasma and a quenching activity toward 4-hydroxy-*trans*-2-nonenal (HNE), chosen as a model of RCS, up to threefold greater than D-carnosine.

Introduction

Reactive carbonyl species (RCS) are important cytotoxic mediators generated by the oxidative damage of biomolecules (that is, lipids, sugars), leading to the alteration of cellular function by signaling to the nucleus, upregulating redox-sensitive transcription factors, and inducing irreversible structural modifications in biomolecules.[1–4] The α,β-unsaturated aldehydes [4-hydroxy-*trans*-2-nonenal (HNE), acrolein (ACR)], and dialdehydes [malondialdehyde (MDA), glyoxal (GO)] are the most abundant and toxic lipid-derived RCS, generated in several pathophysiological conditions through the β-cleavage of hydroperoxides from ω-6 polyunsaturated fatty acids (arachidonic and linoleic acid). RCS are electrophilic and reactive compounds capable of forming covalent adducts with nucleophilic molecules, in particular proteins and nucleic acids.[4] RCS and the related adducts with proteins (that is, carbonylated proteins) are widely used as biomarkers of lipid peroxidation and, in general, of oxidative stress.[5] Moreover, a strict correlation between carbonyl stress and certain human diseases is well established. The accumulation of RCS is recognized as a common feature of aging in tissue proteins, and levels of these compounds are increased either systemically or locally in a broad range of diseases, including diabetes, atherosclerosis, renal, hepatic, and neurodegenerative diseases.[1–4] Whether RCS represent a cause or an effect is still to be fully clarified, although, for some diseases, several convincing evidences support a pathogenic role of RCS, such as in the case of diabetic-related diseases,[6] age-dependent tissue dysfunction,[7] neurodegenerative diseases,[8] and atherosclerosis.[9] Consequently, RCS are predictive biomarkers of oxidative damage and represent biological targets for drug discovery.[10,11]

Taking RCS and carbonylation damage as a drug target, various molecular strategies have been considered to neutralize or decrease these pathogenic factors, and the most promising is based on nucleophilic compounds that detoxify RCS by forming covalent and unreactive adducts (RCS-sequestering agents). Although these compounds belong to different chemical classes, are all characterized by at least one nucleophilic center, such as thiol, imidazole, or primary amine group, responsible for the scavenging effect. Among the sequestering agents recognized to date, the vitamer pyridoxamine (PYR), the vasodilating antihypertensive drugs hydralazine (HY) and dihydralazine (di-HY), the iNOS inhibitor aminoguanidine (AG), and the oral hypoglycemic agent metformin (MF) are the most investigated. Although characterized by high reactivity toward cytotoxic RCS, the clinical application for most of these compounds is limited given their promiscuous activity and lack of selectivity, the latter due to the cross-reactivity with physiological aldehydes, such as pyridoxal (PYAL).[4,10]

[a] *Dr. G. Vistoli, Dr. M. Orioli, Dr. A. Pedretti, Dr. L. Regazzoni, Prof. M. Carini, Prof. G. Aldini*
Dipartimento di Scienze Farmaceutiche "Pietro Pratesi"
Facoltà di Farmacia, Università degli Studi di Milano
Via Mangiagalli 25, 20133 Milano (Italy)
Fax: (+39) 02-5031-19359
E-mail: giancarlo.aldini@unimi.it

[b] *Dr. R. Canevotti, Dr. G. Negrisoli*
Flamma S.p.A., Via Bedeschi 22, Chignolo d'Isola (BG) (Italy)

Supporting information for this article is available on the WWW under http://dx.doi.org/10.1002/cmdc.200800433.

We recently found that L-carnosine (β-alanyl-L-histidine, L-CAR), an endogenous dipeptide present at millimolar concentrations in some tissues, such as the skeletal muscle, is a selective quencher of α,β-unsaturated aldehydes both in vitro and ex vivo conditions.[12] Despite these promising features, the therapeutic use of L-CAR is limited because of its instability in human plasma due to the presence of carnosinase, a specific dipeptidase which catalyzes the hydrolytic cleavage of the dipeptide ($t_{1/2}$ of carnosine in human serum <5 min).[13] In addition, the RCS quenching potency of L-CAR is lower than that of the reference RCS quenchers, such as PYR, AG, and HY. Several carnosine derivatives have been proposed (see the review by Guiotto et al.)[14] for their antioxidant activity. Regarding RCS-sequestering activity, the CAR modifications reported to date concern the substitution of β-alanine with aliphatic residues (that is, valylhistidine, leucylhistidine)[14] and the modification of the amino group of β-alanine with hydrazide and 1,2-diol moieties.[15]

By considering the potential interest of L-CAR as a RCS quencher and, in particular, its high selectivity due to the peculiar quenching mechanism, we undertook a study aimed to rationally design L-CAR derivatives characterized by the following features: 1) resistance to carnosinase; 2) selectivity toward cytotoxic RCS; 3) greater reactivity toward α,β-unsaturated aldehydes than L-CAR.

Among the various strategies to stabilize a peptidic bond, we focused our attention on amino acid isomerization. In particular, the conversion of L- to D-histidine leads to a derivative (β-alanyl-D-histidine, D-carnosine, D-CAR) not recognized by the catalytic site of carnosinase, as rationalized by in silico analysis. D-CAR was found to be stable in human serum for at least 8 h, maintaining the same potency of L-CAR in quenching α,β-unsaturated aldehydes, such as HNE and ACR.[16] Based on these premises, the aim of the present study was the design, synthesis, and evaluation of metabolically stable and selective D-CAR derivatives characterized by an increased reactivity toward α,β-unsaturated aldehydes relative to CAR, using HNE as a prototype RCS.

Rational design of carnosine analogues

To optimize the activity of novel CAR derivatives without decreasing their selectivity, it is worth considering the particular reaction mechanism of CAR with α,β-unsaturated aldehydes. Previously, Zhou and Decker[17] hypothesized that an imidazole group and a primary amine moiety, opportunely spaced, are the minimum structural requirements for CAR reactivity toward α,β-unsaturated aldehydes. The reaction mechanism was then independently elucidated by Aldini et al.[18] and Liu et al.[19] It involves the Schiff base formation between the β-alanine amino group and the aldehyde function, which then catalyzes the Michael adduct formation between the C3 of the aldehyde and the Nτ of the histidine group (Scheme 1) by approaching the two reactive centers. The high selectivity of CAR, as demonstrated for the first time to our knowledge in the study reported herein, is easily explained on the basis of this mechanism of reaction, which avoids cross-reactivity with physiologically relevant carbonyl compounds as a result of the reversibility of the Schiff base in aqueous solutions. Consequently, the optimization of scavenging activity can be achieved by optimizing both the reactions involved.

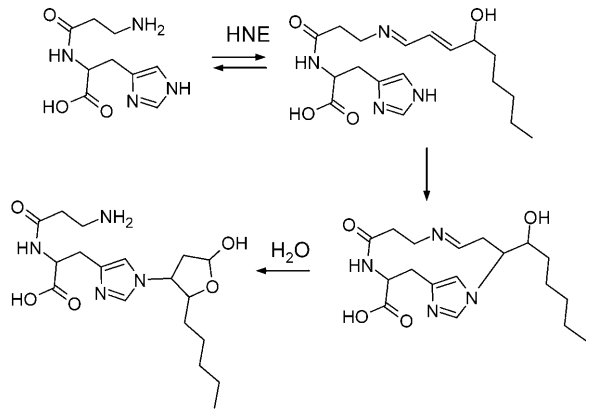

Scheme 1. Proposed reaction mechanism of carnosine with 4-hydroxy-*trans*-2,3-nonenal (HNE).

The modifications of carnosine structure to increase the reactivity of the amino group and promote imine formation are very tricky. Indeed, even considering that polarizability, (de)stabilization of transition states, and solvent effects can abnormally modify the reactivity of an amino group, there is a clear relation between nucleophilicity and basicity.[20] This means that it is virtually impossible to improve the reactivity of a nucleophilic center without increasing its basicity. However, it is well known that the formation of an imine group involves only a fraction of the amine present in the unprotonated form. Paradoxically, a useful approach to enhance the formation of the imine would conversely involve the decrease in the basicity of the amino group, irrespective of its nucleophilicity, even if a marked decrease in basicity could impair the selectivity of novel derivatives. Moreover, CAR derivatives, where the amino group was modified by introducing the hydrazine moiety, have already been described.[15] Hence, our attention was focused on the optimization of the Michael condensation.

The considerations previously mentioned for the amino group also apply to modulation of the reactivity of the imidazole ring. Thus, the imidazole represents a suitable compromise between reactivity and basicity, providing an optimal selectivity to CAR and its derivatives. Indeed, the histidine residue alone is not able to yield the Michael adduct, as previously demonstrated,[18] but requires the previous imine formation, which approaches the imidazole ring to the reactive C3 atom. This implies that the ability of the imine intermediate to assume close conformations leading to Michael adduct is a crucial factor in determining the scavenging activity of such derivatives. Consequently, we focused our attention on the possible modifications of the CAR structure to favor the productive close conformations. Figure 1 summarizes the conformational behavior of the L-CAR–HNE imine adduct, showing that the extended conformers, which are in equilibrium with the folded conformers, represent only half of all monitored geometries. This suggests that the conformational profile of the

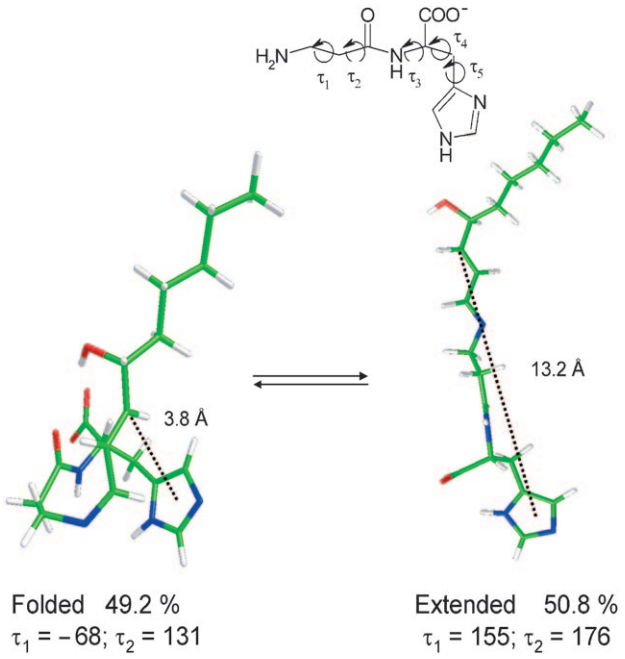

Figure 1. Conformational profile of the imine adduct CAR–HNE, illustrating the equilibrium between folded reactive and extended unreactive conformers. The percentages are computed considering a cutoff distance of 8 Å.

imine intermediates can be largely optimized by suitable modification of the CAR structure to shift this equilibrium toward the folded reactive conformations. Based on these premises, a set of D-CAR derivatives containing aryl moieties substituted in the β-alanine residue (α and β to the amino group) was prepared on solid phase by means of an automatic synthesizer (Table 1). Such modifications only slightly influence the basicity of the amino group (thus avoiding a significant loss of selectivity) and concomitantly should approach the intermediate Schiff base to the imidazole through π–π interactions, thus stabilizing favorable close conformations.

Table 1. Structures of the carnosine derivatives studied, along with AG, HY, and PYR, chosen as reference compounds.

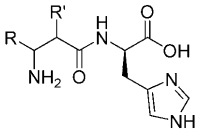

Compd	R	R′
D-CAR	H	H
A-1	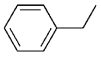	H
A-5	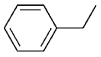	OH
A-7	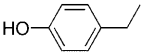	H
A-10	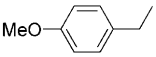	H
A-6		H
A-9	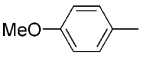	H
A-4	H	Ph
A-2		H
A-11	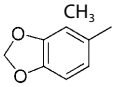	H
aminoguanidine (AG)	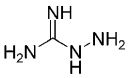	
hydralazine (HY)	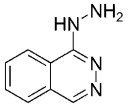	
pyridoxamine (PYR)	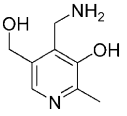	

Results

HNE quenching activity (reactivity)

The HNE quenching ability of CAR derivatives was first evaluated by measuring the aldehyde consumption using HPLC analysis. Table 2 lists the quenching activities of the proposed derivatives (normalized to the activity of CAR) relative to those of the selected reference compounds AG, PYR, and HY. Notably, despite the well-known reactivity of AG toward HNE (leading to the formation of an imine adduct),[21] the quenching activity of AG, as determined by HPLC analysis, was almost negligible. The quenching activity was then tested by a direct infusion MS approach, consisting of the evaluation of the quencher consumption at pH 7.4, with respect to a blank incubated in the absence of the target aldehyde. As, in these conditions, AG was found to be effective, we can reasonably suppose that the acidic mobile phase, by catalyzing the Schiff base decomposition, would be responsible for the negative results obtained working with the HPLC method. The MS method was then extended to all the tested compounds. Unlike AG, the order of potency for CAR derivatives in both the HPLC and MS approaches was found to be the same, as confirmed by the satisfactory linearity between the two sets of data (correlation coefficient $r^2 = 0.95$). This is not surprising considering the structure of the reaction products of CAR derivatives with HNE (Michael adducts, see below), which are stable under the acidic conditions required for HPLC analysis. These results also emphasize the role of MS as an alternative technique to HPLC for in vitro evaluation of the RCS-quenching ability of compounds forming acid-sensitive adducts.

Table 2 clearly shows that some designed modifications to the CAR structure markedly improve the quenching activity relative to the parent compound. In particular, all the derivatives of β3 homophenylalanine and β3 homotyrosine (**A-1**, **A-5**, and **A-10**) showed enhanced activities, the derivatives of β2 and β3 homophenylglycine (**A-4**, **A-6**, **A-9**, and **A-11**) afforded diverse quenching effects possibly depending on stereoelectronic factors, whereas the derivative of β3 homoalanine (**A-2**) yielded very modest activity.

Table 2. Quenching activity, selectivity, and plasma stability of D-CAR, D-CAR derivatives, and reference compounds.

Compd	Quenching Activity[a]		Selectivity [%][b]	Plasma Stability [%][c]
	HPLC	MS		
D-CAR	1	1	102.4 ± 2.9	101.4 ± 4.8
A-10	2.69 ± 0.06	2.73 ± 0.03	98.3 ± 2.4	96.3 ± 4.4
A-7	2.37 ± 0.06	2.15 ± 0.02	99.7 ± 0.8	105.6 ± 7.8
A-1	1.90 ± 0.08	1.98 ± 0.01	97.5 ± 2.7	97.4 ± 4.4
A-4	1.76 ± 0.07	1.56 ± 0.03	102.9 ± 3.2	102.5 ± 3.7
A-6	1.68 ± 0.04	1.58 ± 0.02	100.4 ± 3.2	101.4 ± 2.7
A-5	0.87 ± 0.07	0.98 ± 0.03	97.4 ± 3.1	99.4 ± 2.5
A-9	0.40 ± 0.04	0.63 ± 0.02	98.6 ± 2.9	99.9 ± 3.6
A-2	0.38 ± 0.05	0.43 ± 0.01	103.4 ± 4.3	100.2 ± 4.5
A-11	0.32 ± 0.03	0.45 ± 0.03	99.0 ± 1.4	99.4 ± 4.1
HY	4.66 ± 0.14	4.78 ± 0.09	0	ND
AG	0	3.45 ± 0.08	0	ND
PYR	1.67 ± 0.09	1.78 ± 0.05	0[d]	ND

[a] Results are normalized to the activity of carnosine. [b] Results are reported as the percentage of PYAL remaining relative to a blank incubated in the absence of tested compound. [c] Results are reported as the percentage of the tested compound remaining relative to a blank incubated in the absence of serum (60 min at 37 °C); ND: not determined. [d] Selectivity was determined by MS.

The quenching activity of both novel derivatives and reference compounds was further studied by identifying the reaction products by direct infusion MS analysis in full scan mode. The method was first applied to identify and characterize the reaction products of HNE with AG, PYR, and HY which are summarized in Scheme 2.

Reference compounds–HNE adducts

The mass spectrum of AG solution was characterized by the $[M+H]^+$ at *m/z* 75 (base peak) (data not shown). The incubation with HNE for 3 h induced the formation of the ions at *m/z* 213 (base peak) and at *m/z* 231 (relative abundance 10%), corresponding to the Schiff base and Michael adduct, respectively (Scheme 2a and figure S1A, Supporting Information). After 24 h of incubation, the ion at *m/z* 213 was still the base peak, and the ion at *m/z* 231 increased by almost 20%. Attribution of the Schiff base was confirmed by MS–MS analysis (figure S1B, Supporting Information).

The mass spectrum relative to HY incubated for 3 h and spiked with Tyr-His as internal standard (IS) is characterized by the $[M+H]^+$ ion at *m/z* 319 and *m/z* 161 relative to that of the IS and HY, respectively (data not shown). HNE incubation induced, within three hours, the formation of two additional ionic species at *m/z* 299 and *m/z* 317, with a relative abundance of almost 40%, and attributed to the Michael adduct and Schiff base, respectively (Scheme 2b and figure S2A, Supporting Information). After 24 h incubation, the relative abundance of HY was further decreased to 45%, whereas the ion at *m/z* 299 became the base peak (data not shown). The identity of the adducts was confirmed by MS–MS analyses. The MS–MS data of the ion at *m/z* 299 are characterized by the fragment ions at *m/z* 146 $[Hy+H-NH]^+$, *m/z* 161 $[Hy+H]^+$, and *m/z* 170.9, the latter of which is due to the cleavage between the phthaline nucleus and the hydrazine nitrogen (figure S2B, Supporting Information). The tandem mass spectrum of the adduct at *m/z* 317 was characterized by the ions at *m/z* 161, resulting from a retro-Michael reaction (loss of 156), and at *m/z* 139 $[HNE+H-H_2O]^+$ (figure S2C, Supporting Information).

The mass spectrum of the reaction mixture containing PYR and HNE (3 h incubation) contains, in addition to the $[M+H]^+$ relative to unreacted PYR (*m/z* 169.2), the ion at *m/z* 325 attributed to the $[M+H]^+$ of the Michael adduct (Scheme 2c and figure S3A, Supporting Information). The tandem mass spectrum is dominated by the ion at *m/z* 169, due to a retro-Michael reaction, and at *m/z* 152 (base peak), resulting from the sequential loss of the amine moiety (figure S3B, Supporting Information).

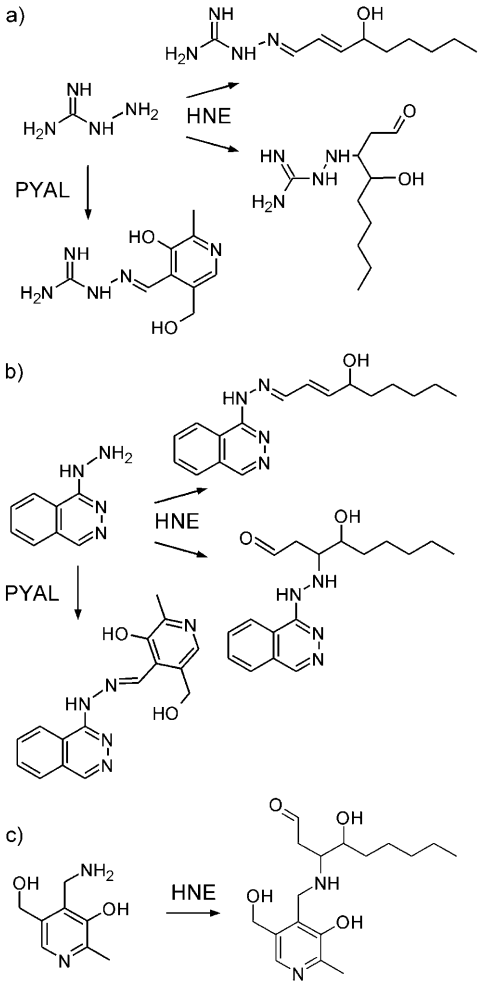

Scheme 2. Reaction products of a) AG, b) HY, and c) PYR with HNE and PYAL.

Carnosine derivatives–HNE adducts

The mass spectrum of D-CAR solution was characterized by an intense $[M+H]^+$ ion at *m/z* 227, and by the corresponding $[M+Na]^+$ adduct at *m/z* 249. The spectrum did not change up to 24 h incubation at 37 °C, indicating the stability of CAR under these conditions. The same behavior was observed for all the CAR derivatives. After incubation of D-CAR with HNE, an intense ion at *m/z* 383 and the corresponding $[M+Na]^+$ adduct at *m/z* 405 were evident, attributed to Michael adduct in the hemiacetal form, as previously reported by us for L-CAR (Scheme 1).[18]

The mass spectra of the CAR derivatives incubated with HNE were all characterized by the presence of the $[M+H]^+$ of the parent compound, and of the corresponding $[M+H+156]^+$ adduct ion, indicating Michael adduct formation, as further confirmed by MS–MS analyses (Table 3). As an example, Figure 2 reports the mass spectrum of compound **A-10** before (panel a) and after reaction with HNE (panel b) for 24 h.

Table 3. Ionic species detected in the MS data.[a]

Compd	Parent $[M+H]^+$	Michael Adduct $[M+H+156]^+$
D-CAR	227.1	383.1
A-10	347.4	503.4
A-7	333.3	489.3
A-1	317.3	473.3
A-4	303.3	459.3
A-6	303.1	459.2
A-5	333	489.3
A-9	333.3	489.3
A-2	240.3	396.3
A-11	346.3	502.3

[a] Recorded (direct infusion) after incubating each CAR derivative with HNE for 24 h.

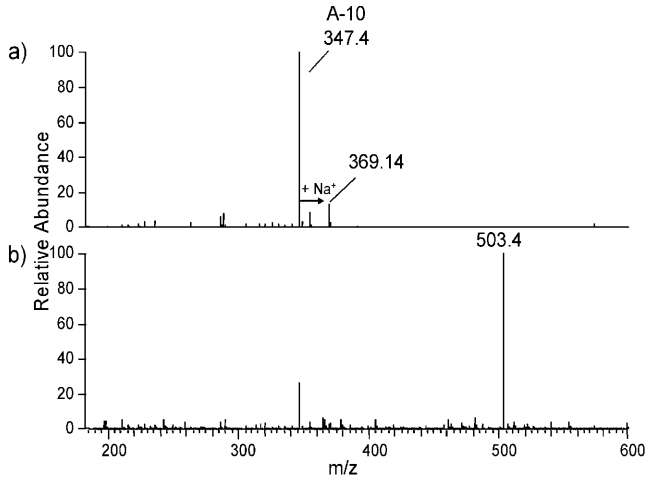

Figure 2. Characterization of the reaction product of **A-10** with HNE. Shown are the MS data for the reaction mixtures after 3 h incubation in the a) absence and b) presence of HNE.

Pyridoxal quenching activity (selectivity)

HPLC analyses indicated that AG and HY induce an almost complete depletion of the physiological aldehyde within 3 h of incubation (Table 2). This lack of selectivity was further confirmed by MS analysis of the incubates, whereby the disappearance of the $[M+H]^+$ signal relative to the quencher was accompanied by the formation of the corresponding reaction product. The mass spectrum of the pyridoxal–aminoguanidine reaction mixture incubated for 24 h shows an abundant ionic species at *m/z* 224 corresponding to the $[M+H]^+$ of the Schiff base between the amino moiety of AG and the carbonyl of PYAL. The attribution was confirmed by the presence, in the MS–MS data, of the fragment ion at *m/z* 165 (base peak), due to the cleavage of the hydrazine moiety (figure S4A, Supporting Information). The mass spectrum of the reaction mixture containing PYAL and HY shows a base peak at *m/z* 310 relative to the $[M+H]^+$ of the PYAL-HY adduct, attributed to the Schiff base (theoretical *m/z* 310.16). The MS–MS data relative to the ion at *m/z* 310 shows as main product ions those at *m/z* 165 (base peak), arising from the cleavage of the hydrazinic bond, and at *m/z* 161 $[HY+H]^+$ (figure S4B, Supporting Information), confirming the structure assignment. The selectivity of PYR, after incubation with PYAL and PYAL phosphate, was studied by measuring the consumption of the quencher using only the MS approach (HPLC analysis was not applicable because of the co-elution of PYR and PYAL). The results were similar to those obtained for AG and HY: a complete depletion of PYR was observed in the presence of both PYAL and PYAL phosphate, indicating the lack of selectivity of the tested compound. In contrast, all the designed CAR derivatives were found to be highly selective. None of them induced a significant consumption of PYAL during 3 h of incubation (HPLC assay), and none of them, when analyzed by direct infusion MS, gave rise to the formation of additional ionic species. The mass spectra of the tested compounds spiked with PYAL were found to be superimposable with those obtained in the absence of the target aldehyde, up to 24 h of incubation (data not shown), thus excluding the formation of any adduct.

Plasma stability

L-CAR incubated in human serum rapidly disappeared, being undetectable after 5 min of incubation, the first time point considered (data not shown). To measure the hydrolysis rate experiments were also performed using suitably diluted serum (1:20). Under these conditions, CAR consumption was significantly decreased ($t_{1/2} = 3$ min), and the calculated hydrolysis rate was 170 nmol mL^{-1} min^{-1}. As shown in Table 2, D-CAR and derivatives were found to be stable in undiluted human serum up to 8 h, where the recovery was not significantly different with respect to a blank incubated in the absence of serum.

Physicochemical profiling

For D-CAR and analogues, Table 4 shows the experimental p*K* values, as determined by potentiometric titration, and the pre-

Table 4. Physicochemical properties[a] and conformational profile[b] for D-CAR and D-CAR derivatives.

Compd	pK_1[c]	pK_2	pK_3	$\log P_{MLP}$[d]	Folded Conformers [%][e]
D-CAR	2.76	9.32	6.72	−4.08	49.8
A-10	2.66	8.78	6.71	−1.59	76.8
A-7	2.63	8.73	6.70	−2.43	62.5
A-1	2.61	8.71	6.71	−1.97	71.5
A-4	2.73	8.94	6.95	−2.53	55.2
A-6	2.74	8.27	6.82	−2.35	53.7
A-5	2.39	8.36	6.85	−2.73	46.4
A-9	2.52	8.47	6.89	−2.20	28.1
A-2	2.71	9.29	6.73	−3.35	43.5
A-11	2.73	8.41	6.86	−3.26	46.3

[a] Ionization constants and computed lipophilicity. [b] Percentage of folded conformers. [c] Constants determined by potentiometric titration. [d] Predicted log*P* values for zwitterionic forms. [e] Percentages derived by MD simulations in water.

dicted log*P* values for the zwitterionic forms as computed by the MLP approach.[22] All considered derivatives possess at least three ionization constants (pK_1 refers to the carboxylic acidity, pK_2 is due to the amino group basicity, and pK_3 is for the imidazole basicity) and **A-7** also has a fourth constant ($pK_4 = 9.98$) attributable to the phenol acidity. The p*K* values for D-CAR were in agreement with those already published for L-CAR.[23]

The analysis of the ionization constants revealed that the designed modifications significantly modify the pK_2 values, whereas pK_1 and pK_3 remain unchanged. In detail, all proposed compounds showed a decrease in amino group basicity with an increased fraction of unprotonated reactive amine and a favorable effect on imine formation. However, as this pK_2 variation was shared by all considered CAR analogues, which show a remarkable variability in their quenching activities, one can conclude that the basicity of the amino group, albeit relevant, does not play a key role and other possible factors must be considered. The calculated log*P* values emphasized the marked hydrophilicity of all D-CAR derivatives, even if all designed modifications decrease the polarity relative to that of D-CAR. There is a modest relation between lipophilicity and quenching activity ($r^2 = 0.45$), although this seems due to the ability of log*P* values to indirectly encode the positive effects of aryl rings rather than an intrinsic role of the lipophilicity itself. Nonetheless, considering the nonpolar nature of HNE, one can also suppose that less polar scavengers could better approach the HNE molecules.

Conformational studies

The conformational profile of carnosine is characterized by five rotatable bonds (Figure 2); the first two torsions (τ_1 and τ_2) concern the backbone of β-alanine, τ_3 involves the histidine backbone, whereas the last two torsions (τ_4 and τ_5) belong to the side chain of histidine. The conformational profile of CAR analogues alone appear clearly frozen by the intramolecular ion pair, whereas the rotors are markedly more flexible in the corresponding imine adducts with HNE. The histidine torsions (τ_3, τ_4, and τ_5) show a marked flexibility in all considered compounds and do not seem to be crucial in determining the global conformation of the imine adducts. Conversely, the β-alanine torsions (τ_1 and τ_2), which are somewhat tethered by the neighboring peptide and imine bonds, play a key role in defining the conformational profile of these adducts. Basically, synclinal geometries in τ_1 and τ_2 favor a productive approaching between the imidazole ring and the HNE C3 center, whereas antiperiplanar conformations move the two reactive centers away, yielding extended conformations which appear unsuited for the Michael adduct formation.

To analyze the ability of such imine derivatives to assume productive conformations (avoiding a systematic analysis of all rotatable bonds) the distance between the imidazole barycenter and the C3 reactive atom was calculated. For each derivative, Table 4 reports the percentage of conformations (as derived by molecular dynamics (MD) runs) with monitored distances of < 8 Å, a value chosen as cutoff to discriminate between reactive and unreactive conformations. Table 4 and Figure 2 reveal a noteworthy relation between the quenching activities and the percentages of folded reactive conformations ($r^2 = 0.78$). This result confirms that the approaching between imidazole and the C3 atom plays a pivotal role in the bioactivity of such carnosine derivatives and suggest that the conformational profile could be successfully exploited to predict the scavenger activity of novel carnosine analogues.

Discussion

RCS generated by the oxidation of biomolecules are electrophilic and cytotoxic compounds involved as pathogenic factors in some human diseases, such as atherosclerosis and diabetic related diseases. RCS and, in general, protein carbonylation are now considered potential drug targets and promising pharmacological effects have been reported by using RCS-sequestering agents; nucleophilic compounds able to detoxify RCS by forming unreactive covalent adducts (an extensive review on the chemistry and biological effects of this class of compounds has been recently published[4]).

AG, HY, and PYR are the most studied RCS-sequestering agents, and their pharmacological activity has already been demonstrated in several animal models.[4] These compounds are characterized by a broad spectrum of scavenging ability toward different classes of reactive carbonyls, as in the case of AG, which is an active scavenger of various α,β-dicarbonyls such as GO, MGO, 3-deoxyglucosone, MDA, and α,β-unsaturated aldehydes.[21,24] The RCS-sequestering activity for this class of compounds is due to the presence of a nucleophilic center, involved in the formation of both a stable Schiff base, by reacting with the aldehyde function, and a Michael adduct, by linking the C3 of the unsaturated aldehyde. Herein, we provided a full MS structure elucidation of the covalent adducts of AG and HY with HNE which is the most abundant α,β-unsaturated aldehyde generated under oxidative stress conditions.[2] The quenching mechanism involves both a Schiff base and Michael adduct formation for HY and AG, and a Michael reaction for

PYR. The high nucleophilicity of the amino group of these compounds, accompanied by a lower basicity which favors the unprotonated form, confers a high reactivity toward a broad range of RCS, but, at the same time, greatly decreases their selectivity making them able to react with biogenic and physiological aldehydes, such as pyridoxal phosphate. The ability of AG, HY, and PYR to quench pyridoxal has been fully clarified, providing elucidation of the structures of the corresponding adducts. In particular, HY (containing a strong nucleophilic hydrazine group) and AG quench PYR by forming a stable Schiff base. PYR is claimed to be selective (and therefore able to spare the endogenous levels of pyridoxal phosphate) on the basis of previous results obtained by HPLC measuring the consumption of the aldehyde using an acid mobile phase.[25] However, by using an MS approach, we observed the depletion of PYR when incubated in the presence of PYAL or PYAL phosphate. These conflicting results could be explained by supposing that a Schiff base is formed, which is unstable in the acidic mobile phase, as we observed for the Schiff base of AG with HNE. Unfortunately, no adducts between PYR and PYAL were detected in the MS conditions we used, and hence further studies are required to better understand PYR selectivity.

The lack of selectivity and the promiscuous activity of the currently available RCS-sequestering compounds represent the main limiting factors for their clinical application, making them practically useless, especially in view of the fact that RCS-mediated diseases are chronic states requiring prolonged treatment for beneficial outcomes. For example, AG has proven to be unsuitable for clinical use, not only because of its inhibitory effect on inducible nitric oxide synthase, but also because of its ability to induce in vivo a significant decrease in the hepatic pyridoxal phosphate content.[26]

We recently found that L-CAR, an endogenous histidine dipeptide, is a selective sequestering agent of α,β-unsaturated aldehydes.[18] The carbonyl sequestering effect has been demonstrated in vitro, in biological matrices, and in ex vivo experiments, using Zucker rats as an animal model of in vivo oxidative damage and protein carbonylation.[12] However, the potential clinical application for this peptide is poor, given the presence of serum carnosinase, a specific dipeptidase which catalyzes the hydrolysis of the peptide. The conversion of L- to D-histidine leads to a derivative (D-CAR) characterized by a high serum stability and a quenching ability similar to that of L-CAR. However, the reactivity of D-CAR is significantly lower than that of the reference compounds, and hence there is an increasing demand for more effective sequestering agents toward α,β-unsaturated aldehydes, which maintains the same selectivity as carnosine.

When discussing the factors that inspired the design of more effective carnosine derivatives, we mainly considered 1) the basicity of amino groups that govern imine formation and 2) the ability to assume folded conformers that promote the Michael adduct reaction. The obtained results reveal a precise role for these factors. Thus, the basicity appears not to be crucial in determining the quenching activity as there is no correlation between bioactivities and pK_2 values. Probably, the high basicity contributes to the poor activity of β3 homoalanine derivative (**A-2**), but it does not seem to be a determinant factor. Conversely, the conformational profile appears to be key factor to enhance the quenching activity by promoting the reaction between imidazole and the C3 atom as evidenced by remarkable correlation between bioactivity and the percentage of folded geometries (Figure 3).

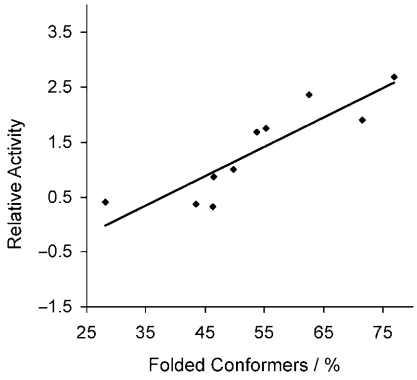

Figure 3. The high correlation ($r^2 = 0.78$) between quenching activity and percentage of folded geometries.

The derivatives of β3 homophenylalanine (**A-1**, **A-5**, and **A-10**) are all more potent than D-carnosine because they favor the close conformation due to the π–π contacts between imidazole and phenyl ring. This is also confirmed by the beneficial effects of electron donor substituents. The different quenching activities of derivatives of β2 and β3 homophenylglycine (**A-4**, **A-6**, **A-9**, **A-11**) can be less easily rationalized because of, for example, the modest activity of *para*-methoxy analogue (**A-9**). Probably, the accessibility of the amino group plays a relevant role in these derivatives as suggested by the very low activity of **A-11**.

In summary, the aryl substitution of D-carnosine appears a fertile strategy to develop efficient RCS quenchers characterized by 1) high selectivity toward physiological aldehydes and 2) plasma stability. Physicochemical profiling and modeling studies underscore the important role of Michael adduct formation and suggest that the abundance of folded conformations can be a successful descriptor to predict and rationalize the activity of novel sequestering agents. For analogy with natural peptides and for synthetic accessibility, we considered only the *S* isomers in the chiral β-alanine moieties in this first study, but the promising results described herein has prompted us to explore the stereoselectivity effects on quenching activity in subsequent studies.

Experimental Section

Synthesis

The synthesis of dipeptide compounds was performed on solid phase by means of an automatic synthesizer. Fmoc-D-His(Trt)-OH is produced by Flamma S.p.A., all the other building blocks are commercially available as are the coupling agents. Process control and HPLC analysis of the final compounds was performed on Agilent

1100 equipment. ^{1}H and ^{13}C NMR were performed on a Bruker 300 Advance instrument.

General procedure for the solid-phase synthesis of the dipeptide derivatives: Fmoc-D-His(Trt)-OH (1.2 equiv) is coupled to a chlorotrityl-polystyrene resin in *N*,*N*-dimethylformamide (DMF) in the presence of *N*,*N*-diisopropylethylamine (DIPEA, 3 equiv). The Fmoc group is removed by two treatments with a solution of piperidine/DMF (25:75) for 15 min. A solution of the suitable Boc-amino acid (2 equiv), PyBOP (2 equiv), and HOBT (2 equiv) in DMF is then added to the reactor containing the resin, followed by DIPEA (5 equiv). The completion of the reaction is monitored by the Kaiser test. After suitable washing, the peptide is cleaved from resin using a solution of trifluoroacetic acid containing 5% H_2O in CH_2Cl_2. The crude peptide is recovered from the solution by precipitation using a suitable solvent, usually an ether. The crude peptide is then purified by preparative HPLC using reversed-phase columns and elution with mixtures of H_2O and CH_3CN. The fractions containing the pure product are concentrated to remove CH_3CN and then freeze-dried to obtain the solid product. Following this procedure, the following compounds have been prepared:

(3*S*)-3-Amino-4-(phenylbutanoyl)-D-histidine (A-1): ^{1}H NMR ([D$_6$]DMSO): δ = 8.35 (bd, J = 7.8 Hz, 1H), 7.58 (d, J = 1.2 Hz, 1H), 5.34 (m, 5H), 6.83 (d, J = 0.6 Hz, 1H), 4.25 (m, 1H), 3.65 (m, 1H), 3.19–3.13 (dd, J = 3.9 Hz, 1H), 3.00–2.90 (dd, J = 4.8 Hz, 1H), 2.80 (m, 2H), 2.42–2.38 (dd, J = 4.2 Hz, 1H), 2.31–2.23 ppm (m, 1H); ^{13}C NMR ([D$_6$]DMSO): δ = 174.79, 172.55, 169.55, 137.49, 134.97, 129.91, 128.96, 127.12, 55.55, 50.83, 29.29, 21.65 ppm.

(3*S*)-3-(Aminobutanoyl)-D-histidine (A-2): ^{1}H NMR (D$_2$O): δ = 8.38 (s, 1H), 7.19 (s, 1H), 4.48 (m, 1H), 3.68 (m, 1H), 3.25–3.20 (dd, J = 5.4 Hz, 1H), 3.09–3.04 (dd, J = 5.1 Hz, 1H), 2.69–2.52 (m, 2H), 1.26 ppm (d, J = 8.7 Hz, 3H); ^{13}C NMR (D$_2$O): δ = 181.27, 176.65, 171.19, 133.67, 130.37, 116.83, 54.23, 44.87, 38.97, 27.47, 23.19, 17.52 ppm.

3-Amino-2-(*S*)-(phenylpropanoyl)-D-histidine (A-4): ^{1}H NMR ([D$_6$]DMSO): δ = 8.80 (bs, 1H), 7.72 (bm, 2H), 7.32 (m, 5H), 7.18 (bs, 1H), 6.83 (s, 1H), 4.51–4.70 (m, 1H), 3.82 (m, 1H), 3.35 (bm, 1H), 3.18–3.05 (m, 2H), 2.87 ppm (m, 1H); MS: $[M+H]^+$ m/z 303.2.

(2*R*,3*S*)-3-Amino-2-hydroxy-4-(phenylbutanoyl)-D-histidine (A-5): ^{1}H NMR ([D$_6$]DMSO): δ = 8.20–8.18 (d, J = 7.5 Hz, 1H), 7.65 (s, 1H), 7.40–7.28 (m, 5H), 6.89 (s, 1H), 4.38–4.32 (s, 1H), 4.20–419 (d, J = 2.7 Hz, 1H), 3.59 (bs, 1H), 3.13–2.80 ppm (m, 4H); ^{13}C NMR ([D$_6$]DMSO): δ = 172.53, 170.88, 137.50, 135.14, 134.18, 129.93, 128.89, 127.05, 117.35, 71.19, 56.30, 54.04, 34.32, 28.95 ppm.

(3*S*)-3-Amino-3-(phenylpropanoyl)-D-histidine (A-6): ^{1}H NMR ([D$_6$]DMSO): δ = 8.47–8.45 (d, J = 8.1 Hz, 1H), 7.69 (s, 1H), 7.55–7.41 (m, 5H), 6.88 (s, 1H), 4.69–4.65 (t, J = 7.2 Hz, 1H), 4.38–4.34 (m, 1H), 3.15–3.08 (dd, J = 4.2 Hz, 1H), 2.90–2.73 ppm (m, 3H); ^{13}C NMR ([D$_6$]DMSO): δ = 172.54, 168.80, 138.27, 135.01, 134.08, 129.16, 128.96, 127.48, 117.13, 54.05, 52.22, 41.12, 29.30 ppm.

(3*S*)-3-Amino-4-(4-hydroxyphenyl)butanoyl-D-histidine (A-7): ^{1}H NMR ([D$_6$]DMSO): δ = 8.37 (d, J = 7.8 Hz, 1H), 7.63 (s, 1H), 7.09 (d, J = 8.6 Hz, 2H), 6.87 (s, 1H), 6.80 (d, J = 8.6 Hz, 2H), 4.37–4.30 (m, 1H), 3.60–3.57 (m, 1H), 3.16–3.10 (dd, J = 4.2 Hz, 1H), 2.95–2.67 (m, 3H), 2.47–2.41 (dd, J = 4.2 Hz, 1H), 2.37–2.29 ppm (dd, J = 7.8 Hz, 1H); ^{13}C NMR ([D$_6$]DMSO): δ = 174.40, 172.50, 169.59, 156.75, 135.07, 134.37, 130.85, 126.83, 117.59, 115.85, 54.74, 50.81, 29.26, 21.60 ppm.

(3*S*)-3-Amino-3-(4-metoxyphenyl)propanoyl-D-histidine (A-9): ^{1}H NMR (D$_2$O): δ = 7.81 (s, 1H), 7.45 (d, J = 7.6 Hz, 2H), 7.17 (d, J = 7.6 Hz, 2H), 6.92 (s, 1H), 4.67 (m, 1H), 4.48 (m, 1H), 4.02 (s, 3H), 3.25–2.82 (m, 5H), 1.48 ppm (d, J = 4.2 Hz, 1H); MS: $[M+H]^+$ m/z 333.1.

(3*S*)-3-Amino-4-(4-methoxyphenyl)butanoyl-D-histidine (A-10): ^{1}H NMR ([D$_6$]DMSO): δ = 8.37 (d, J = 8.6 Hz, 1H), 7.63 (s, 1H), 7.19 (d, J = 8.5 Hz, 2H), 6.87 (s, 1H), 6.71 (d, J = 8.5 Hz, 2H), 4.37–4.30 (m, 1H), 3.98 (s, 3H), 3.60–3.57 (m, 1H), 3.14–3.08 (dd, J = 4.3 Hz, 1H), 2.95–2.81 (m, 2H), 2.75–2.67 (m, 1H), 2.47–2.29 ppm (m, 2H).

(3*S*)-3-Amino-3-(3,4-methylenedioxyphenyl)propanoyl-D-histidine (A-11): ^{1}H NMR ([D$_6$]DMSO): δ = 8.01 (s, 1H), 7.59 (s, 1H), 6.95 (s, 1H), 6.89 (m, 2H), 5.90 (dd, J = 1.2 Hz, 2H), 4.98 (m, 1H), 4.32 (m, 1H), 3.15 (dd, J = 5.1 Hz, 1H), 3.02 (dd, J = 5.0 Hz, 1H), 2.95 (dd, J = 9.2 Hz, 1H), 2.83 ppm (dd, J = 9.1 Hz, 1H).

Reactivity and selectivity

HPLC studies: The reactivity of each carbonyl quencher toward HNE (quenching activity) was evaluated by measuring the HNE consumption (50 μM in 10 mM PBS, pH 7.4) in the presence of the tested compound (1 mM) at a fixed incubation time (60 min, T = 37 °C). The results are normalized to the activity of carnosine, taking the value of 1 as the quenching efficacy afforded by carnosine. HNE consumption was determined by HPLC as reported in the Supporting Information.

Selectivity after three hours of incubation was determined in a similar manner with the exception that PYAL was used as target aldehyde. PYAL consumption was determined by HPLC using a fluorimetric detector as previously reported.[25] The results are reported as percentage of the free aldehyde remaining with respect to a blank incubated in the absence of the tested compound. Structure characterization of the adducts was determined by MS studies after 24 h of incubation (see below).

MS studies: The solutions of each tested compound (final concentration 800 μM in 1 mM phosphate buffer, pH 7.4) were mixed (1:1 *v/v*) with an equimolar concentration of the target aldehyde (HNE or PYAL in 1 mM phosphate buffer, pH 7.4). After incubation at 37 °C for 3 h, the reaction mixtures were spiked with 33 μL of H-Tyr-His-OH (internal standard, 12 mM in 1 mM PBS pH 7.4). An aliquot of the mixture was then diluted 1:4 (*v/v*) with H_2O/CH_3CN (70:30 *v/v*) and analyzed by direct infusion MS as reported in the Supporting Information. The quenching ability of each tested compound (TC) toward HNE or pyridoxal was evaluated by measuring the TC consumption with respect to a blank incubated in the absence of the target aldehyde and using the following equation: quenching activity (%) = [(TC1−TC2)/TC1]×100 for which TC1 and TC2 are the ratio between the current ion intensity of the tested compound and that of the IS in the samples incubated in the presence and absence of the target aldehyde, respectively. MS characterization of the reaction products between PYAL and the tested compound was carried out after 24 h incubation.

Serum stability: Serum stability was evaluated by incubating the TC (50 μM final concentration) in human serum from healthy donors (30–40 years) for 60 min at 37 °C. Aliquots of 100 μL were withdrawn after 5 min and then every 10 min for 60 min, spiked with the IS (Tyr-His, 50 μM final concentration), deprotonated by perchloric acid (PCA, 700 mM final concentration), and centrifuged at 18000 rpm (30000 *g*) for 10 min. The supernatants were then diluted 1:1 with mobile phase A (CH_3CN/H_2O/heptafluorobutyric acid 90:10:0.1 *v/v/v*), filtered through 0.2 μm filters, and then injected into the LC–MS system. Experimental details are reported in the Supporting Information. The results are reported as percentage re-

maining of the tested compound with respect to a blank incubated in the absence of serum. The serum content of each carbonyl quencher was determined by recording the single ion traces (SICs) relative to the $[M+H]^+$ in positive ion mode and using Tyr-His as internal standard.

Reaction product identification by direct infusion MS and MS–MS experiments: Reaction mixtures containing equimolar concentration of the target aldehyde (HNE or pyridoxal) and of each TC (800 μM in 1 mM PBS) were incubated for 24 h at 37 °C. An aliquot (200 μL) of the mixture was then diluted 1:4 (*v*/*v*) with H_2O/CH_3CN (70:30 *v*/*v*) and analyzed by direct infusion on a triple-quadrupole (TQ) mass spectrometer (Finnigan TSQ Quantum Ultra, ThermoQuest, Milan, Italy) equipped with an electrospray ion max source, in both positive and negative ion mode. Identification of the reaction products was carried out in full scan mode (*m*/*z* 50–1500 scan range) and MS–MS data were recorded by setting Q1 and Q3 at a resolution of *m*/*z* 0.7, and by using the optimized collision energy of 35 V.

Determination of ionization constants: The ionization constants of CAR analogues were determined at 25 °C by potentiometric titration using a Sirius GlPKa apparatus (Sirius Analytical Instruments Ltd., Forest Row, East Sussex, UK). All experiments were carried out under a slow N_2 flow to avoid CO_2 absorption. A weighted sample (2–10 mg) was supplied manually; the diluent and all the other reagents were added automatically. In detail, the examined compounds were solubilized in 0.15 M KCl (to adjust the ionic strength) and acidified with 0.1 M HCl to pH 1.8. The solutions were then titrated with standardized KOH to pH 12.2. Bjerrum difference plots were deduced from each titration and used to calculate precise p*K* values. The detailed experimental procedures, data analyses, and the recommended apparatus standardization can be found elsewhere.[27]

Molecular modeling: The imine adducts between HNE and the CAR derivatives were built and minimized in their ionized form as this is the most probable form at the physiological pH. Their conformational profile was explored by a Monte Carlo simulation, as implemented in the VEGA program,[28] which generates 1000 conformers by randomly rotating the rotors. All geometries thus obtained were optimized and clustered according to similarity to discard redundant ones; in detail, two geometries were considered as nonredundant if they differed by more than 60° in at least one torsion angle. The lowest-energy conformer was then inserted in a 20 Å radius cluster of water molecules. After a preliminary minimization to optimize the relative solvent positions, the obtained systems underwent 5 ns of MD simulations using the Namd program.[29] The MD runs had the following characteristics: constant temperature in the range of 300 ± 25 K, integration of Newton's equation every 1 fs according to Verlet's algorithm, spherical boundary condition (radius = 20 Å) applied to stabilize solvent clusters, and frame stored every 5000 iterations (5.0 ps), yielding 6000 frames per trajectory. The MD were carried out in two phases: an initial period of heating from 0 to 300 K over 6000 iterations (6 ps, that is, 1 K per 20 iterations), and the monitored phase of simulation of 5 ns. Only the frames memorized during this last phase were considered. The same Monte Carlo procedure was also exploited to analyze the conformational profile of the considered derivatives alone (that is, without imine adduct) in their zwitterionic form.

Acknowledgements

This work was supported by funds from the University of Milan (PUR 2007, 2008) and from MIUR (PRIN 2007).

Keywords: carnosine · mass spectrometry · molecular modeling · RCS-sequestering agents · reactive carbonyl species

[1] I. Dalle-Donne, G. Aldini, M. Carini, R. Colombo, R. Rossi, A. Milzani, *J. Cell. Mol. Med.* **2006**, 10, 389–406.
[2] G. Poli, R. J. Schaur, W. G. Siems, G. Leonarduzzi, *Med. Res. Rev.* **2008**, *28*, 569–631.
[3] P. J. O'Brien, A. G. Siraki, N. Shangari, *Crit. Rev. Toxicol.* **2005**, 35, 609–662.
[4] G. Aldini, I. Dalle-Donne, R. M. Facino, A. Milzani, M. Carini, *Med. Res. Rev.* **2007**, *27*, 817–868.
[5] N. Zarkovic, *Mol. Aspects Med.* **2003**, *24*, 281–291.
[6] S. Pennathur, J. W. Heinecke, *Antioxid. Redox Signaling* **2007**, *9*, 955–969.
[7] T. Nyström, *EMBO J.* **2005**, *24*, 1311–1317.
[8] R. M. LoPachin, D. S. Barber, T. Gavin, *Toxicol. Sci.* **2008**, *104*, 235–249.
[9] K. Uchida, *Free Radical Biol. Med.* **2000**, 28, 1685–1696.
[10] G. Aldini, I. Dalle-Donne, R. Colombo, R. Maffei Facino, A. Milzani, M. Carini, *ChemMedChem* **2006**, *1*, 1045–1058.
[11] A. Negre-Salvayre, C. Coatrieux, C. Ingueneau, R. Salvayre, *Br. J. Pharmacol.* **2008**, *153*, 6–20.
[12] M. Orioli, G. Aldini, M. C. Benfatto, R. M. Facino, M. Carini, *Anal. Chem.* **2007**, *79*, 9174–9184.
[13] G. Vistoli, A. Pedretti, M. Cattaneo, G. Aldini, B. Testa, *J. Med. Chem.* **2006**, *49*, 3269–3277.
[14] A. Guiotto, A. Calderan, P. Ruzza, G. Borin, *Curr. Med. Chem.* **2005**, 12, 2293–2315.
[15] A. Guiotto, A. Calderan, P. Ruzza, A. Osler, C. Rubini, D. G. Jo, M. P. Mattson, G. Borin, *J. Med. Chem.* **2005**, *48*, 6156–6161.
[16] G. Aldini, R. Canevotti, G. Negrisoli, *Compositions Containing D-Carnosine*, EP1761272 (A1), **2007**.
[17] S. Zhou, E. A. Decker, *J. Agric. Food Chem.* **1999**, *47*, 51–55.
[18] G. Aldini, M. Carini, G. Beretta, S. Bradamante, R. M. Facino, *Biochem. Biophys. Res. Commun.* **2002**, *298*, 699–706.
[19] Y. Liu, G. Xu, L. M. Sayre, *Chem. Res. Toxicol.* **2003**, *16*, 1589–1597.
[20] J. O. Edwards, R. G. Paerson, *J. Am. Chem. Soc.* **1961**, *83*, 16–24.
[21] Y. Al-Abed, R. Bucala, *Chem. Res. Toxicol.* **1997**, *10*, 875–879.
[22] P. Gaillard, P. A. Carrupt, B. Testa, A. Boudon, *J. Comput.-Aided Mol. Des.* **1994**, *8*, 83–96.
[23] C. U. Nielsen, C. T. Supuran, A. Scozzafava, S. Frokjaer, B. Steffansen, B. Brodin, *Pharm. Res.* **2002**, *19*, 1337–1344.
[24] P. J. Thornalley, A. Yurek-George, O. K. Argirov, *Biochem. Pharmacol.* **2000**, *60*, 55–65.
[25] T. Miyata, C. van Ypersele de Strihou, Y. Ueda, K. Ichimori, R. Inagi, H. Onogi, N. Ishikawa, M. Nangaku, K. Kurokawa, *J. Am. Soc. Nephrol.* **2002**, *13*, 2478–2487.
[26] T. Taguchi, M. Sugiura, Y. Hamada, I. Miwa, *Biochem. Pharmacol.* **1998**, *55*, 1667–1671.
[27] A. Avdeef, *J. Pharm. Sci.* **1993**, *82*, 183–190.
[28] A. Pedretti, L. Villa, G. Vistoli, *J. Mol. Graph. Model.* **2002**, *21*, 47–49.
[29] J. C. Phillips, R. Braun, W. Wang, J. Gumbart, E. Tajkhorshid, E. Villa, C. Chipot, R. D. Skeel, L. Kale, K. Schulten, *J. Comput. Chem.* **2005** *26*, 1781–1802.

Received: December 15, 2008
Revised: February 5, 2009
Published online on ■■ ■■, 2009

G. Vistoli, M. Orioli, A. Pedretti,
L. Regazzoni, R. Canevotti, G. Negrisoli,
*M. Carini, G. Aldini**

■■ – ■■

Design, Synthesis, and Evaluation of Carnosine Derivatives as Selective and Efficient Sequestering Agents of Cytotoxic Reactive Carbonyl Species

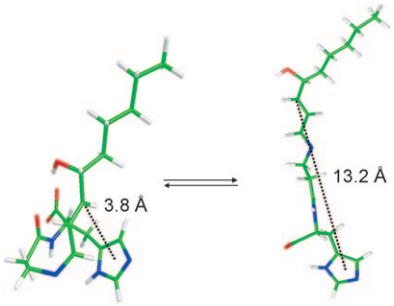

Carnosine aryl derivatives as sequestering agents of RCS: Reactive carbonyl species (RCS) are cytotoxic mediators representing a novel drug target, as they are presumed to play a pathogenic role in several diseases. Carnosine is a selective RCS-sequestering agent, but is rapidly hydrolyzed by serum carnosinase. Herein we describe the in silico design, synthesis, and evaluation of a set of carnosine aryl derivatives.

